

# Photonic Modulation Using Antimony-Trisulphide Phase Change Huygens Metasurfaces

Siddharth Padmanabha<sup>1\*</sup>, Isaac O. Oguntoye<sup>1</sup>, Jesse Frantz<sup>2</sup>, Jason Myers<sup>2</sup>, Robel Bekele<sup>3</sup>, and Anthony Clabeau<sup>3</sup>, Matthew D. Escarra<sup>1</sup>

<sup>1</sup>Department of Physics and Engineering Physics, Tulane University, New Orleans, LA 70118, USA

<sup>2</sup>US Naval Research Laboratory, 4555 Overlook Ave., SW, Washington DC 20375, USA

<sup>3</sup>University Research Foundation, Greenbelt, MD 20770, USA

\* [spadmanabha@tulane.edu](mailto:spadmanabha@tulane.edu)

**Abstract:** We design switchable antimony trisulfide ( $\text{Sb}_2\text{S}_3$ ) Huygens metasurfaces for optical modulation. Simulation results show near  $2\pi$  phase modulation with  $\sim 15\text{dB}$  amplitude modulation optimizable by spectral resonance tuning at near infrared wavelengths. Experimental verification is in progress.

© 2021 Optical Society of America

**OCIS codes:** 160.0160(Materials) 160.3918(Metamaterials) 130.4110 (Modulators)

## 1. Introduction

Reconfigurable photonic devices are highly desirable for their use in data storage and optical communication, optical metrology, optical displays and more [1, 2]. Phase change materials (PCMs) provide the opportunity for the design of such devices using their changes in optical properties when switched from different volatile or non-volatile phases. Many current non-volatile PCM devices are designed around germanium-antimony-tellurium (GST) and operate in the mid-IR region.  $\text{Sb}_2\text{S}_3$  provides the unique opportunity to do the same in the visible and near-IR regions with potential for very low optical loss [1].

At near-IR wavelengths around 700-800 nm,  $\text{Sb}_2\text{S}_3$  exhibits a refractive index contrast of 0.75 with low loss ( $k < 0.01$ ) when switched between its crystalline and amorphous phases [3]. Such switching may be accomplished by thermal, optothermal or electrical methods. This switching can be exploited to design Huygens source optical nanoradiators for reconfigurable optical modulation. Huygens metasurfaces utilize spectrally overlapping magnetic and electric resonances, which through careful selection of geometry, can achieve  $2\pi$  phase tuning around the spectral resonance locations with high transmissivity. The geometry of these metasurfaces can be further tuned to achieve spectrally adjacent electric and magnetic resonances, which result in reflectance peaks and present a wider spectral range over which phase and amplitude modulation can be achieved. Amplitude modulation can be achieved through absorption or reflectance modulation. At lower wavelengths, specifically between 620-720 nm, the crystalline  $\text{Sb}_2\text{S}_3$  phase is lossy, while the amorphous phase is near lossless. While at higher wavelengths, the refractive index contrast can be exploited to design reflectance peak shifts with minimal absorption. With heterogenous antenna arrays, these desirable properties can be utilized to design a wide range of photonic structures and behaviors.

## 2. Modulator Design and Fabrication

### 2.1 Design and Modeling

The geometry of Huygens sources as low aspect ratio  $\text{Sb}_2\text{S}_3$  nano-discs in a periodic arrangement (Figure 1A) was optimized to create spectrally overlapping resonant metasurfaces for near IR wavelengths in the crystalline phase ( $\lambda = 780$  nm). An encapsulating layer of polydimethylsiloxane (PDMS) is used to protect the metasurfaces from physical damage while creating an index match with the antennas' quartz substrate. These metasurfaces, when switched from the crystalline to the amorphous phase, display a resonance blue shift of about 100 nm (Figure 1B). This resonance shift results in a phase modulation of  $\sim 310$  degrees at a minimal amplitude modulation of  $\sim 0.5\text{dB}$  at  $\lambda = 720$  nm, while amplitude modulation of  $\sim 15\text{dB}$  at a phase shift of  $\sim 100$  degrees is observed at  $\lambda = 620$  nm (Figure 1C).

Similar designs were optimized for spectrally adjacent resonances with a spectral peak separation of  $\sim 80$  nm between the electric and magnetic field resonant peaks. Switching these metasurfaces results in a resonance peak shift of 150 nm for the B field peak and 90 nm for the E field peak (Figure 1D). These resonance shifts result in a phase modulation of  $\sim 265$  degrees with minimal amplitude modulation of  $\sim 0.14$  dB at  $\lambda = 950$  nm (Figure 1E). Efforts to optimize these designs to create modulators with full  $2\pi$  phase shift and larger amplitude modulation are underway.

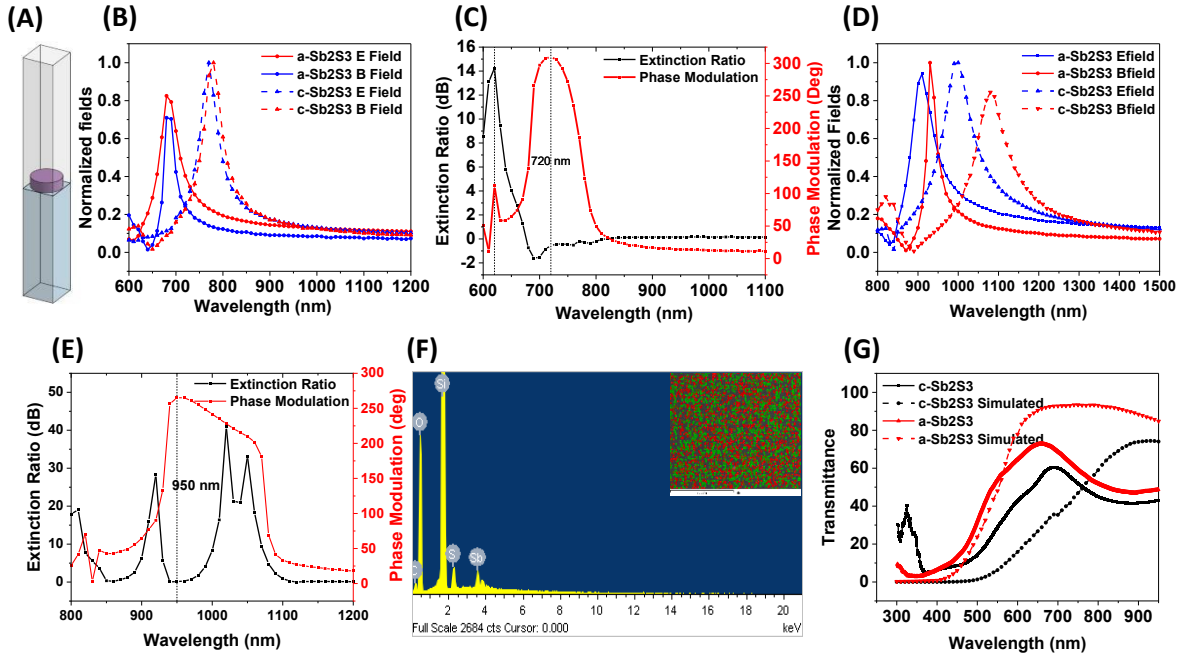


Figure 1: (A)  $\text{Sb}_2\text{S}_3$  Huygens metasurface unit cell, with PDMS encapsulant domain and quartz substrate domain; (B) Normalized electric and magnetic field intensities confined within the nanoantennas for amorphous (a-) and crystalline (c-) nanoantennas featuring spectrally overlapping resonances (diameter = 262.5 nm, edge-to-edge spacing = 160 nm, height = 120 nm); (C) Phase and amplitude modulation vs. wavelength for antenna array in (B); (D) Field intensities in the nanoantennas for spectrally adjacent resonance design (diameter = 330 nm, edge-to-edge spacing = 251 nm, height = 195 nm); (E) Phase and amplitude modulation for the antenna array in (D); (F) EDS data for  $\text{Sb}_2\text{S}_3$  thin films sputtered at 100°C, with inset showing Sb-S spatial profile (red = Sb, yellow = S, green = Sb+S overlap); (G) Transmittance data comparison between experimental and simulated films. Films coated with 120nm  $\text{SiO}_2$  capping layer were crystallized on a hot plate at 300°C for 10 minutes.

## 2.2 Fabrication and Characterization

$\text{Sb}_2\text{S}_3$  thin films are created by RF Magnetron sputtering with in situ substrate heating. Current films show a transmittance trend comparable to published literature [4] and simulation data (Figure 1G). To prevent the lateral migration of Sulphur [5] and oxidation in air during phase change, a 120 nm  $\text{SiO}_2$  capping layer is deposited. Electron dispersive spectroscopy (EDS) data show excess sulfur content in the films (Figure 1F). Excess sulfur can be mitigated by increasing the substrate temperature during sputtering and by ex situ annealing. Film synthesis is currently being optimized, with feedback from ongoing stoichiometric, crystal structure, and optical property and performance analysis. Thermal and optical switching methods are being tested, and a nanofabrication plan has been formulated.

## 3. Conclusion

Design and modeling of a PDMS-capped  $\text{Sb}_2\text{S}_3$  metasurface for optical modulation has been achieved. Simulation results show a near  $2\pi$  phase shift and  $\sim 0.5\text{dB}$  amplitude modulation at 720 nm using spectrally overlapping resonances and a  $1.5\pi$  phase shift with minimal amplitude modulation for spectrally adjacent resonances at 950 nm. Additionally,  $\sim 15\text{dB}$  amplitude modulation with  $\pi/2$  phase shift has been achieved at 620 nm. Thin film synthesis is being optimized as we prepare to fabricate and characterize these switchable  $\text{Sb}_2\text{S}_3$  metasurface designs.

***This work is supported in part by the National Science Foundation (DMR-1654765 and DMR-1727000).***

## References

- [1] M. Wuttig, et. al, "Phase-change materials for non-volatile photonic applications," in *Nature Photonics*, 2017.
- [2] G. Liang, H. Huang, et. al, "Efficient Pure Phase Optical Modulator Based on Strongly Over-Coupled Resonators," in *CLEO*, San Jose, 2019.
- [3] Weiling Dong, et. al, "Wide Bandgap Phase Change Material Tuned Visible Photonics," in *Adv. Functional Materials*, 2019.
- [4] M. Calixto-Rodriguez, et. al, "A comparative study of the physical properties of  $\text{Sb}_2\text{S}_3$  thin films treated with  $\text{N}_2$  AC plasma and thermal annealing in  $\text{N}_2$ ," in *Applied Surface Science*, vol. 256, no. 8, pp. 2428-2433, 2010.
- [5] M. Delaney, et. al, "A New Family of Ultralow Loss Reversible Phase-Change Materials for Photonic Integrated Circuits:  $\text{Sb}_2\text{S}_3$  and  $\text{Sb}_2\text{Se}_3$ ," in *Adv. Functional Materials*, vol. 30, no. 36, 2020.